Articles

Asymmetry of Catalytic but Not of Noncatalytic Sites on *Escherichia coli* F_1-ATPase in Solution As Observed Using Electron Spin Resonance Spectroscopy†

Ralf M. Lösel, John G. Wise, and Pia D. Vogel*

Fachbereich Chemie der Universität Kaiserlautern, Erwin-Schrödinger Strasse, 67663 Kaiserslautern, Germany

Received June 19, 1996; Revised Manuscript Received November 20, 1996⊗

ABSTRACT: We have employed electron spin resonance (ESR) spectroscopy using different spin-labeled nucleotides to probe the environment of nucleotides bound at catalytic and noncatalytic nucleotide binding sites of the *Escherichia coli* F_1-ATPase. We found that nucleotides bound in the noncatalytic binding sites were strongly immobilized and resulted in ESR spectra with one single corresponding spectral component. Nucleotide bound at the catalytic binding sites gave rise to two different signals in the ESR spectra indicative of two distinct conformations of the catalytic sites of the protein. One conformation of the catalytic sites is very tight, resulting in signals identical to those of the noncatalytic sites, while the second type of catalytic sites permitted an unusually high mobility of the bound spin-labeled nucleotide. The findings are compared to the requirements of the binding change mechanism and to the features of the nucleotide binding sites as elucidated from the X-ray structural model of the beef heart mitochondrial enzyme.

F_oF_1 ATP synthases catalyze the terminal step in oxidative phosphorylation or photophosphorylation, i.e. the reaction of inorganic phosphate (P_i) with adenosine diphosphate (ADP) to form adenosine triphosphate (ATP), making use of the energy inherent in a proton gradient across the membrane in which the enzyme is embedded [for reviews, see Senior (1990), Penefsky and Cross (1991), and Boyer (1993)]. The enzyme is located in the bacterial cytoplasmic membrane, the inner mitochondrial membrane, and the thylakoid membranes of chloroplasts.

The structure of F_oF_1 ATP synthase is complex, consisting of the membrane-spanning F_o part that forms the pathway for protons through the membrane and the F_1 portion, which is peripherally bound to the membrane-embedded F_o. The simplest ATP synthase is found in *Escherichia coli* and other bacteria and exhibits a subunit stoichiometry of $\alpha_3\beta_3\gamma\delta\epsilon ab_{1-2}c_{10-12}$ (Foster & Fillingame, 1982). Convincing evidence has been accumulated that shows that F_1-ATPases from beef heart mitochondria (MF_1), chloroplasts (CF_1), and *E. coli* (EF_1) contain a total of six nucleotide binding sites (Cross & Nalin, 1982; Wise *et al*., 1983; Xue *et al*., 1987). X-ray crystallographic studies support this contention, although only five nucleotides were bound to the crystallized F_1 (Abrahams *et al.*, 1994).

On the basis of the rate of exchange of protein-bound nucleotide with medium nucleotide under turnover conditions, three of the binding sites have been termed potential catalytic sites (Cross & Nalin, 1982). The remaining three binding sites exchange nucleotides too slowly to participate in catalysis and are therefore called noncatalytic binding sites. Their function is not yet clear.

Noncatalytic binding sites were for a long time assumed to be specific for adenine nucleotides in contrast to catalytic sites, which bind guanosine and inosine-derived nucleotides rather nonspecifically (Harris, 1978; Perlin *et al.*, 1984). More recent investigations have shown, however, that GTP can bind to noncatalytic sites of CF_1, MF_1, and EF_1 (Guerrero *et al*., 1990; Milgrom & Cross, 1993; Weber *et al*., 1994; Hyndman *et al*., 1994). GDP in contrast exhibited only negligible binding to EF_1 (Weber *et al*., 1994).

In the X-ray structural model of MF_1-ATPase (Abrahams *et al*., 1994), asymmetry was observed within the catalytic binding sites. The different conformations of the binding sites correlate nicely to the different structures that are required by the binding change mechanism [see Boyer (1993)]. Crystallization was carried out in the presence of ADP and an excess of the nonhydrolyzable ATP analog, AMPPNP. The crystals contained ADP, AMPPNP, or no nucleotide bound to the β-subunits. The possibility that the asymmetry observed is at least partially induced by the binding of different nucleotides to the binding sites cannot be ruled out. In addition, the resulting enzyme with AMPPNP and ADP bound to catalytic sites was most likely in a form that would show inhibited ATP hydrolysis. We thought it would be informative to investigate whether active F_1-ATPase in solution would also exhibit asymmetry in the nucleotide binding site conformations.

Electron spin resonance (ESR) spectroscopy has proven to be a valuable tool for investigating protein structures, with even small changes of intramolecular or segmental flexibility being detectable. Besides the use of spin-labels covalently attached to proteins (Morisett, 1976), spin-labeled substrates and cofactors have often been employed successfully to

† This project was funded by a grant from the Deutsche Forschungsgemeinschaft to P.D.V.

* To whom correspondence should be addressed. Phone: (49) 631-205-3801. Fax: (49) 631-205-3419. E-mail: vogel@chemie.uni-kl.de.

⊗ Abstract published in *Advance ACS Abstracts,* January 1, 1997.

S0006-2960(96)01460-2 CCC: $14.00

obtain information about structure in or near active sites [for reviews, see Trommer (1987), Park and Trommer (1989), and Trommer and Vogel (1992)]. Spin-labeled ATP analogs like 2′,3′-SL-ATP[1] and derivatives thereof have been used before to study ATPases (Vogel-Claude *et al.*, 1988; Vogel *et al*., 1992; Burgard *et al*., 1993; Lösel *et al*., 1996). The corresponding 2-N_3-SL-ATP has been shown to occupy the same binding sites and label the same amino acid residues as 2-N_3-ATP (Vogel *et al.*, 1992). In this paper, we have made use of spin-labeled nucleotides and used ESR spectroscopy to determine structural differences within the nucleotide binding sites of *E. coli* F_1 in solution.

MATERIALS AND METHODS

Protein. The *E. coli* strain used (SWM1; Rao *et al*., 1988) was a gift from A. E. Senior, University of Rochester, Rochester, NY. The cells were grown on a supplemented minimal medium containing chloramphenicol (15 μg/mL) as described by Wise (1990). Cultures of 500 mL (Erlenmeyer flasks aerated by rotation) or 12 L (New Brunswick Scientific Microferm fermenter) were harvested by centrifugation in the late exponential phase, and F_1-ATPase was isolated by a modification of the method of Wise (1990) that substituted a Q-Sepharose anion exchange column (Pharmacia, 15 × 150 mm) for the Millipore DEAE-5PW HPLC column. The ATP hydrolysis activities were in the range of 20−34 u/mg.

Nucleotide Analogs. 2-N_3-SL-ATP was synthesized essentially as described (Czarnecki, 1984; Melese & Boyer, 1985; Jakobs *et al*., 1989). SL-GDP was prepared from the corresponding guanine nucleotide as described for the ATP analog (Streckenbach *et al.*, 1980; Vogel-Claude *et al*., 1987).

ESR Measurements. The ESR spectra were recorded on a Bruker ESP 300 E spectrometer operating in the X-band mode. Flat quartz cuvettes (50 μL) were used in a TE_{102} resonator. The spectra were recorded at 298 K with a scan range of 120 G, a microwave power of 20 mW, and a peak to peak modulation amplitude of 0.8 G. If necessary for better visualization of the signals of immobilized radicals, the spectra were re-recorded at increased signal gain. Enzyme samples were prepared for ESR experiments by concentrating the F_1 solutions in Centricon 30 concentrators (Amicon) and desalting the F_1 by two passages through centrifuge columns [Penefsky, 1977; Sephadex G-50 (Pharmacia), equilibrated with 50 mM Tris-HCl at pH 8.0]. The amount of spin-labeled nucleotide bound to the enzyme was measured as the difference between the known total concentration of nucleotide added to the ESR cuvette and the free nucleotide observed. The free nucleotide was measured by comparing the signal amplitude of the high-field signal of the unbound, freely tumbling nucleotide spin-label to a standard curve generated without enzyme. The experiments were performed by adding a premixed solution of 2-N_3-SL-ATP and $MgCl_2$ (2.5:1) to the enzyme.

Nucleotide Depletion. F_1-ATPase was depleted of endogenous nucleotides by column chromatography on Sephadex G-50 in buffer containing 50% glycerol essentially as described by Garrett and Penefsky (1975) [see Wise *et al*. (1983) and Senior *et al.* (1992)]. Enzyme fractions were concentrated using Centricon 30 concentrators and were either used directly or stored in 50% glycerol buffer at −70 °C.

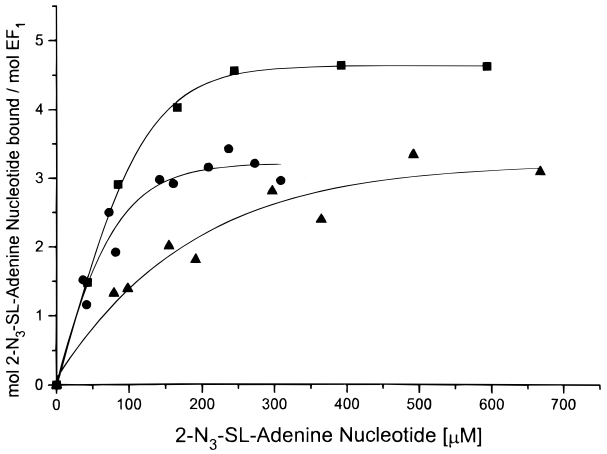

FIGURE 1: Concentration dependence of spin-labeled nucleotide binding to F_1. (●) Native F_1-ATPase was incubated at a starting concentration of 35 μM in buffer containing 50 mM Tris-Cl at pH 8.0. 2-N_3-SL-ATP was added stepwise to give the concentrations indicated. Mg^{2+} ions were supplemented to give a nucleotide to Mg^{2+} ratio of 2.5:1 for all experiments described. (▲) Native F_1-ATPase was incubated at starting concentrations of 44 or 23 μM (two individual experiments) as above, except that SL-AMPPNP was added. (■) Nucleotide-depleted F_1-ATPase was incubated at a starting concentration of 35 μM with various concentrations of 2-N_3-SL-ATP as above.

Routine Analysis. Protein concentrations were determined according to the method of Bradford (1976) using defatted bovine serum albumin (Boehringer) as a standard. ATP hydrolysis was assayed at 25 °C and pH 8 with 1−5 μg of enzyme as described by Wise *et al.* (1981). The production of inorganic phosphate was detected by the method of Taussky and Shorr (1953). The purity of the protein was routinely assayed by SDS−PAGE (Laemmli, 1970).

RESULTS

Figure 1 shows the binding of 2-N_3-SL-ATP in the dark (circles) and the nonhydrolyzable analog SL-AMPPNP (triangles) to *E. coli* F_1-ATPase that had not been previously depleted of its endogenous nucleotides (native F_1). Maximal binding was reached at about 3 mol/mol in both cases. Binding of the 2-N_3-SL-ATP was almost stoichiometric with the added nucleotide until the nucleotide concentration exceeded the high protein concentration required for ESR measurements. Such observations suggest that the dissociation constants for the first sites filled are well below the nucleotide concentrations used in Figure 1. Binding of the SL-AMPPNP analog to native F_1 was weaker than that of 2-N_3-SL-ATP. At the protein concentrations used, half-maximal binding was reached at an approximately 130 μM total SL-AMPPNP concentration. Binding of 2-N_3-SL-ATP to nucleotide-depleted F_1-ATPase resulted in maximum binding of almost 5 mole of nucleotide analog per mol of F_1 (squares). Again, the binding was almost stoichiometric in the lower concentration range, suggestive of dissociation constants well below the protein concentrations used in these experiments.

[1] Abbreviations: 2′,3′-SL-ATP, 2′,3′-(2,2,5,5-tetramethyl-3-pyrroline-1-oxyl-3-carboxylic acid ester) ATP (2′,3′ indicates a rapid equilibrium of the ester bond between C2′ and C3′ of the ribose moiety); 2-N_3-SL-ATP, 2-azido-2′,3′-(2,2,5,5-tetramethyl-3-pyrroline-1-oxyl-3-carboxylic acid ester) ATP; ANP, adenine nucleotide with an undefined number of phosphoryl groups.

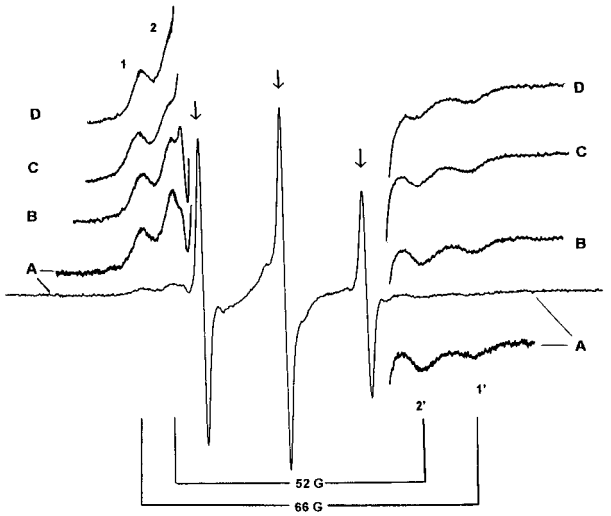

FIGURE 2: ESR spectra of native F_1-ATPase in complex with increasing concentrations of 2-N_3-SL-ATP. (A) F_1 (35 μM) was incubated with 2-N_3-SL-ATP (36 μM) as described for Figure 1. The low- and high-field regions were re-recorded at higher signal gain for better visualization of the signals: (B) 34 μM F_1 in the presence of 72 μM 2-N_3-SL-ATP, (C) 34 μM F_1 in the presence of 141 μM 2-N_3-SL-ATP, and (D) 33 μM F_1 in the presence of 272 μM 2-N_3-SL-ATP.

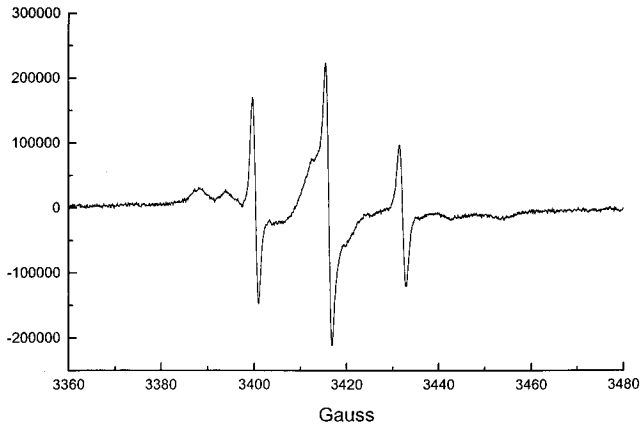

FIGURE 3: ESR spectra of F_1 in complex with SL-AMPPNP. F_1 (24 μM) was incubated with SL-AMPPNP (98 μM) as described for Figure 1. The spectrum was recorded digitally, and multiple scans increased the signal to noise ratio.

The ESR spectra of F_1-ATPase in the presence of different concentrations of 2-N_3-SL-ATP are shown in Figure 2. Even at the lowest concentration used (35 μM F_1 and 36 μM 2-N_3-SL-ATP), two clearly separated signals derived from enzyme-bound radicals are visible with $2A_{zz}$ values of 52 and 66 G. In addition, the signals of the non-enzyme-bound (free) SL-ANP are visible as the sharp signals marked by arrows.

To test whether the two different environments of protein-bound spin-label were due to enzymatic hydrolysis of the ATP analog used in the previous experiment, we employed the nonhydrolyzable derivative of ATP, SL-AMPPNP, for further investigations. In Figure 3, the corresponding ESR spectrum is shown. Again, there are clearly two signals, 1,1′ and 2,2′, visible with $2A_{zz}$ values of 66 and 52 G, respectively, indicating that also under conditions where the nucleotide is not hydrolyzed two different types of conformationally different binding sites exist on F_1-ATPase.

Addition of unlabeled ATP/Mg^{2+} at a ratio of 2.5:1 under turnover conditions to F_1-ATPase that had been incubated with excess 2-N_3-SL-ATP/Mg^{2+} (like in Figure 2) resulted in ESR spectra as shown in Figure 4. Only the signals with a $2A_{zz}$ value of 66 G are visible, in addition to the signals of the free nucleotide analog (arrows), while the 52 G signal was not observed in these samples after ATP hydrolysis.

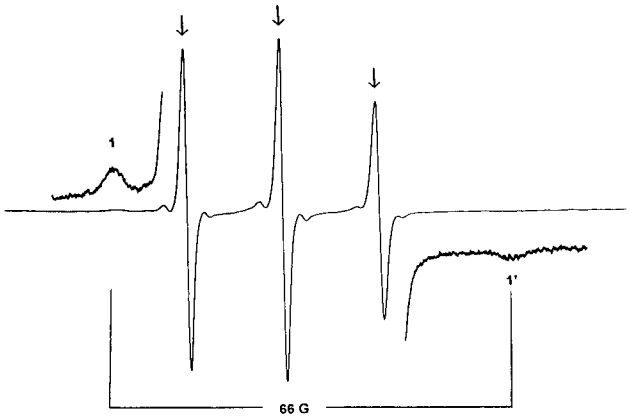

FIGURE 4: ESR spectra of F_1 in complex with 2-N_3-SL-ATP after ATP addition. F_1 (37 μM) was incubated with 2-N_3-SL-ATP (300 μM) as in Figure 1. After removal of excess nucleotide by passage through a centrifuge column, ATP and $MgCl_2$ were added to final concentrations of 3.6 and 1.4 mM, respectively. The ESR spectrum was recorded directly after mixing. The low- and high-field regions were re-recorded at higher signal gain for better visualization of the signals.

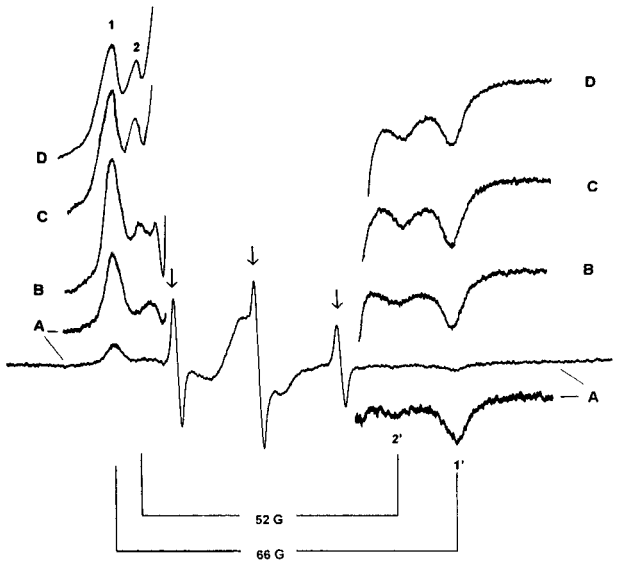

FIGURE 5: ESR spectra of nucleotide-depleted F_1-ATPase in complex with increasing concentrations of 2-N_3-SL-ATP. (A) Nucleotide-depleted F_1 (23 μM) was incubated with 2-N_3-SL-ATP (42 μM) as in Figure 1. The low- and high-field regions were re-recorded at higher signal gain to allow better visualization of the signals: (B) 35 μM F_1 in the presence of 84 μM 2-N_3-SL-ATP, (C) 34 μM F_1 in the presence of 165 μM 2-N_3-SL-ATP, and (D) 33 μM F_1 in the presence of 390 μM 2-N_3-SL-ATP.

The ESR spectra of nucleotide-depleted F_1-ATPase in the presence of different concentrations of 2-N_3-SL-ATP are shown in Figure 5. Both spectral components with $2A_{zz}$ values of 52 and 66 G are visible in addition to the sharp signals of the unbound spin-labeled nucleotides (arrows). Under these conditions, the signal of the highly immobilized radical component (66 G) dominates the spectrum at the lower nucleotide concentrations (compare spectra A and B of Figure 5 to spectra A and B of Figure 2).

After acquisition of the spectrum shown in Figure 5D, excess free nucleotide analog was removed from the protein

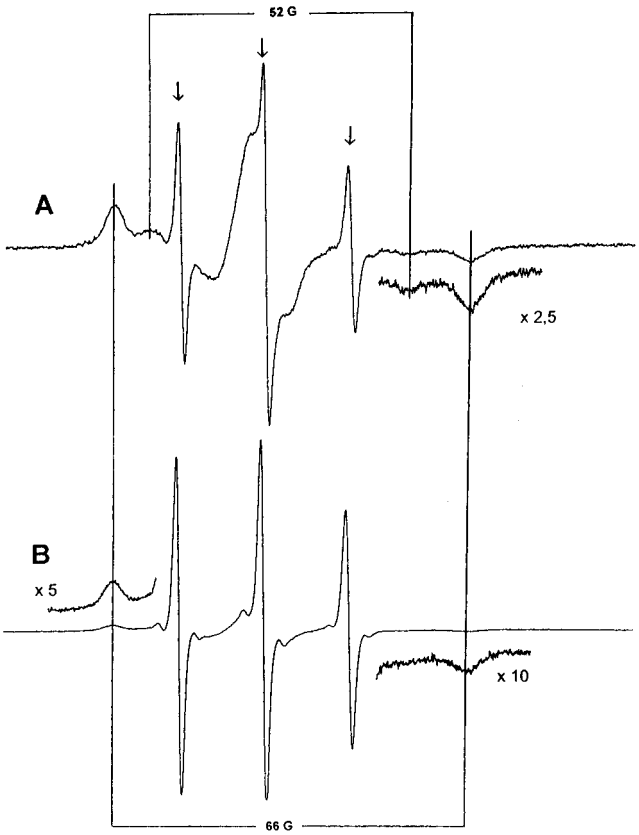

FIGURE 6: ESR spectra of nucleotide-depleted F_1 in complex with 2-N_3-SL-ATP after GDP exchange. (A) F_1-ATPase that was incubated with 2-N_3-SL-ATP under the conditions as described for Figure 4D was passed through a centrifuge column. The small amount of remaining free label is marked by arrows. (B) ESR spectrum of the sample from part A after addition of GDP to a final concentration of 10 mM. The low- and high-field regions were re-recorded at higher signal gain for better visualization of the signals.

solution using the centrifuge column technique. The resulting spectrum is shown in Figure 6A. Again, the two different spectral components are visible in addition to the spectrum of approximately 3−5% of free 2-N_3-SL-ANP that overlays the middle part of the spectra (arrows). Addition of GDP to a concentration of 10 mM to the cuvette resulted in ESR spectra as shown in Figure 6B. Only the 66 G signal remains under such conditions; the 52 G signal was not observed after incubation with GDP.

DISCUSSION

The binding curves shown in Figure 1 show distinct differences in binding stoichiometry and affinity that were dependent on the presence or absence of intrinsic nucleotides in the F_1-ATPase preparation and the nucleotide analog used. Approximately two additional 2-N_3-SL-ANPs were bound to nucleotide-depleted enzyme compared to native enzyme that still contained intrinsic nucleotides.

The ESR spectra of native F_1-ATPase in the presence of various amounts of 2-N_3-SL-ATP are shown in Figure 2A−D. Two distinct signals of protein-immobilized spin-labeled nucleotides are clearly visible (1,1′ and 2,2′). The middle part of the spectra is overlaid by the stronger signals of the freely tumbling non-enzyme-bound 2-N_3-SL-ANP. The outer pair of signals, 1,1′, with a $2A_{zz}$ value of 66 G can be explained by binding of the spin-labeled ANP to a binding site that creates an environment that leads to strong immobilization of the radical. The inner signal pair (2,2′) however, exhibits a $2A_{zz}$ value of only 52 G and must arise from radicals that possess a far higher degree of mobility within the binding site. The difference of 14 G between the $2A_{zz}$ values for 1,1′ and signal 2,2′ is very large and is strong evidence for great differences within the respective environments (conformations of binding sites). No dipolar spin interactions were observed in our experiments using *E. coli* F_1-ATPase that would indicate two spin-labeled nucleotides bound to the enzyme in close vicinity.

One possible explanation for the observed ESR spectra is that, upon hydrolysis of the 2-N_3-SL-ATP, the corresponding SL-ADP analog ($\pm P_i$) may have bound in a different conformation to F_1 than the SL-ATP. This could be due to the loss of binding constraints from one phosphoryl group upon hydrolysis. Less spatial restraints on the SL-ADP analog may have resulted in higher mobility of the radical within the binding site which might give rise to the signals with the unusually low $2A_{zz}$ value of 52 G. We used the spin-labeled analog of the nonhydrolyzable ATP analog, SL-AMPPNP, to test this theory. Maximal binding of SL-AMPPNP was reached at about 3 mol/mol for the native enzyme (see Figure 1, triangles), a value similar to the one obtained with the ATP analog itself. Binding was weaker as can be seen by the half-maximal binding concentration of about 130 μM. The ESR spectra of F_1 in complex with SL-AMPPNP were identical in shape to those observed with 2-N_3-SL-ATP (Figure 3). Both signals of the enzyme-immobilized components with the $2A_{zz}$ values of 66 and 52 G were observed. These data show that the different environments of the radical components that give rise to the different signals are not due to differences in binding of 2-N_3-SL-ATP and the corresponding 2-N_3-SL-ADP analog. In addition, since the SL-AMPPNP does not contain an azido group, the possibility that the known equilibrium of the 2-azido function with the corresponding tautomeric tetrazole forms (Czarnecki, 1984) was responsible for the differences within the ESR spectra can be ruled out.

We also synthesized and tested SL-ATP derivatives that have the spin-label fixed in either the 2′- or the 3′-position of the ribose (2′-deoxy-3′-SL-ATP and 2′-SL-3′-deoxy-ATP) to test if the 2′−3′ equilibrium of the ribose-modified nucleotides (Streckenbach *et al.*, 1980) was responsible for the different spectral components. We found in all cases, however, two signals with $2A_{zz}$ values similar to the ones described above (C. Motz, unpublished observations).

A fourth possible explanation for the occurrence of the two distinctly different signals in the ESR spectrum is that the catalytic and noncatalytic binding sites have conformations that differ significantly from each other in solution or that there are strong structural differences within the same type of binding sites as was seen for the catalytic binding sites in the X-ray structural model presented by Abrahams *et al.* (1994).

Covalent incorporation of 2-N_3-SL-ANP could theoretically answer this question. Unfortunately, the 2-azido function of 2-N_3-SL-ATP could not be used to its full capabilities here. Experiments showed that, after photolysis of 2-N_3-SL-ANP bound to F_1 and subsequent passage through a centrifuge column, the 52 G signal diminished over time, indicating that the ANP analog did not covalently incorporate into these binding sites. It was therefore impossible to identify the binding sites through analysis of

the labeled amino acids. In earlier work, we showed that 2-N_3-SL-ATP covalently modified both catalytic and noncatalytic nucleotide binding sites of the mitochondrial F_1-ATPase (Vogel *et al.*, 1992). Covalent incorporation in such experiments is never quantitative, and we can therefore not rule out the fact that certain conformations of catalytic and/or noncatalytic sites may not have been modified by the reagent.

Another useful method for distinguishing between nucleotides bound at catalytic and noncatalytic binding sites is based on the difference in exchangeability of bound nucleotide with medium nucleotide. Brief catalytic turnover normally results in the exchange of the nucleotides bound to the catalytic sites, while the nucleotides bound to noncatalytic binding sites remain bound under such conditions. This method has been successfully used to specifically modifiy catalytic and noncatalyitc nucleotide binding sites on *E. coli* F_1-ATPase using 2-N_3-ATP (Wise *et al.*, 1987). We used these characteristics to differentiate the origins of the different signals by adding an excess of unlabeled MgATP under V_{max} conditions to F_1-ATPase that had been previously incubated with 2-N_3-SL-ATP. We observed complete disappearance of the inner 52 G signal upon addition of the normal substrate. The outer 66 G signal remained clearly visible, although its intensity had slightly decreased (see Figure 4). It was clear from independent measurements of ATP hydrolysis activities under the conditions used for our ESR experiments that no inhibited state of the enzyme existed that would leave SL-ANP bound to the catalytic sites. These findings suggest that the inner 52 G signal and parts of the outer 66 G signal may represent catalytic sites in different conformational states and that the outer signal may also arise from SL nucleotides bound to noncatalytic sites. The fact that the MgATP used to remove SL-ANP from exchangeable sites binds to both catalytic and noncatalytic sites, however, makes these findings somewhat ambiguous.

Further evidence that at least part of the outer signal (1,1′) is due to occupation of noncatalytic sites with 2-N_3-SL-ANP was achieved in the experiment shown in Figure 5 where we used F_1-ATPase that had been depleted of intrinsic nucleotides. The outer 66 G signal is clearly dominant relative to the 52 G signals, indicating that more of the sites leading to the 66 G signals were occupied. The binding curve (see Figure 1) also shows additional binding of two nucleotide analogs compared to the native enzyme. Since the slowly exchanging nucleotides in F_1-ATPases that are removed during the procedure to nucleotide-deplete the protein are mostly nucleotides bound to noncatalytic sites (Kironde & Cross, 1986), the increase of the 66 G signal suggests that it in part arises when SL nucleotides bind to noncatalytic sites.

Weber *et al*. (1994a) demonstrated for mutants where tryptophan had been substituted for residues in the noncatalytic binding sites that GDP did not bind significantly to noncatalytic sites. To be able to use this property to distinguish between catalytic and noncatalytic sites, we added an excess of GDP to a sample of nucleotide-depleted F_1 that had been saturated with 2-N_3-SL-ATP and passed through a centrifuge column to remove unbound nucleotides (see Figure 6A). The ESR spectrum after GDP addition shows that the 52 G signal had totally disappeared, while the outer 66 G signal remained but was weaker in intensity (see Figure 6B). This experiment strongly supports the hypothesis that both catalytic and noncatalytic binding sites in complex with SL-ANP give rise to the outer 66 G signal, while the inner 52 G signal represents spin-labeled adenine nucleotides bound to catalytic sites in a very different conformation.

We also synthesized and employed SL-GDP in our studies, reasoning that the GDP analog should bind exclusively to catalytic sites. Binding of SL-GDP to F_1 was very weak. At the concentrations used in the experiments, only the 66 G signal was clearly visible. This experiment strongly supports the theory that the 66 G signal is at least in part derived from nucleotide binding to catalytic sites.

ACKNOWLEDGMENTS

The authors thank A. E. Senior (University of Rochester) for providing *E. coli* strain SWM1 and T. Schanding and S. Burgard (Universität Kaiserslautern, Germany) for SL-GTP and SL-AMPPNP, respectively. We also express our gratitude to W. E. Trommer for his support.

REFERENCES

Abrahams, J. P., Leslie, A. G. W., Lutter, R., & Walker, J. E. (1994) *Nature 370*, 621−628.

Bianchet, M., Yserm, X., Hullihen, J., Pedersen, P. L., & Amzel, L. M. (1991) *J. Biol. Chem. 266*, 21197−21201.

Boyer, P. D. (1993) *Biochim. Biophys. Acta 1140*, 215−250.

Bradford, M. M. (1976) *Anal. Biochem. 72*, 248−254.

Burgard, S., Nett, J. H., Sauer, H. E., Kagawa, Y., Schäfer, H.-J., Wise, J. G., Vogel, P. D., & Trommer, W. E. (1994) *J. Biol. Chem. 269*, 17815−17819.

Cross, R. L., & Nalin, C. M. (1982) *J. Biol. Chem. 257*, 2874−2881.

Czarnecki, J. J. (1984) *Biochim. Biophys. Acta 800*, 41−51.

Foster, D. L., & Fillingame, R. H. (1982) *J. Biol. Chem. 257*, 2009−2015.

Garrett, N. E., & Penefsky, H. S. (1975) *J. Biol. Chem. 250*, 6640−6647.

Guerrero, K. J., Ehler, L. L., & Boyer, P. D. (1990) *FEBS Lett. 270*, 187−190.

Harris, D. A. (1978) *Biochim. Biophys. Acta 463*, 245−273.

Hyndman, D. J., Milgrom, Y. M., Bramhall, E. A., & Cross, R. L. (1994) *J. Biol. Chem. 269*, 28871−28877.

Jakobs, P., Sauer, H. E., McIntyre, J. O., Fleischer, S., & Trommer, W. E. (1989) *FEBS Lett. 254*, 8−12.

Kironde, F. A. S., & Cross, R. L. (1986) *J. Biol. Chem. 261*, 12544−12549.

Laemmli, U. K. (1970) *Nature 227*, 680−685.

Lösel, R. M., Erbse, A. H., Nett, J. H., Wise, J. G., Berger, G., Girault, G., & Vogel, P. D. (1996) *Spectrochim. Acta, Part A 52*, 73−83.

Melese, T., & Boyer, P. D. (1985) *J. Biol. Chem. 260*, 15398−15401.

Milgrom, Y. M., & Cross, R. L. (1993) *J. Biol. Chem. 268*, 23179−23185.

Morisett, J. D. (1976) in *Spin Labeling, Theory and Applications* (Berliner, L. J., Ed.) pp 273−338, Academic Press, Inc., New York.

Park, J. H., & Trommer, W. E. (1989) in *Biological Magnetic Resonance* (Berliner, L. J., & Reuben, J., Eds.) Vol. 8, pp 547−595, Plenum Publishing Corp., New York.

Penefsky, H. S. (1977) *J. Biol. Chem. 252*, 2891−2899.

Penefsky, H. S., & Cross, R. L. (1991) *Adv. Enzymol. Relat. Areas Mol. Biol. 64*, 173−214.

Perlin, D. S., Latchney, R. L., Wise, J. G., & Senior, A. E. (1984) *Biochemistry 23*, 4998−5003.

Rao, R., Al-Shawi, M. K., & Senior, A. E. (1988) *J. Biol. Chem. 263*, 5569−5573.

Senior, A. E. (1990) *Annu. Rev. Biophys. Chem. 19*, 7−41.

Senior, A. E., Lee, R. S. F., Al-Shawi, M. K., & Weber, J. (1992) *Arch. Biochem. Biophys. 297*, 340−344.
Streckenbach, B., Schwarz, D., & Repke, K. H. R. (1980) *Biochim. Biophys. Acta 601*, 34−46.
Taussky, H. H., & Schorr, E. (1953) *J. Biol. Chem. 202*, 675−685.
Trommer, W. E. (1987) in *Pyridine Nucleotide Coenzymes: Chemical, Biochemical and Medical Aspects* (Dolphin, D., Poulson, R., & Avramovic, O., Eds.) Vol. 2a, pp 613−639, Wiley, New York.
Trommer, W. E., & Vogel, P. D. (1992) in *Bioactive Spin Labels* (Zhdanov, R. I., Ed.) pp 405−428, Springer-Verlag Berlin, Heidelberg.
Vogel, P. D., Nett, J. H., Sauer, H. E., Schmadel, K., Cross, R. L., & Trommer, W. E. (1992) *J. Biol. Chem. 267*, 11982−11986.
Vogel-Claude, P., Schäfer, G., & Trommer, W. E. (1988) *FEBS Lett. 227*, 107−109.
Weber, J., Wilke-Mounts, S., Grell, E., & Senior, A. E. (1994) *J. Biol. Chem. 269*, 11261−11268.
Wise, J. G. (1990) *J. Biol. Chem. 265*, 10403−10409.
Wise, J. G., Latchney, L. R., & Senior, A. E. (1981) *J. Biol. Chem. 256*, 10383−10389.
Wise, J. G., Duncan, T. M., Latchney, L. R., Cox, D. N., & Senior, A. E. (1983) *Biochem. J. 215*, 343−350.
Wise, J. G., Hicke, B. J., & Boyer, P. D. (1987) *FEBS Lett. 223*, 395−401.
Xue, Z., Zhou, J.-M., Melese, T., Cross, R. L., & Boyer, P. D. (1987) *Biochemistry 26*, 3749−3753.

BI9614601